Available online at www.sciencedirect.com
ScienceDirect
Catalysis Today 122 (2007) 186–194
CATALYSIS TODAY
www.elsevier.com/locate/cattod

Oxidation of acetylene by photocatalysis coupled with dielectric barrier discharge

F. Thevenet [a,b], O. Guaitella [b], E. Puzenat [a], J.-M. Herrmann [a], A. Rousseau [b], C. Guillard [a,*]

[a] *Laboratoire d'Application de la Chimie à l'Environnement, UMR-CNRS 5634, Université-Lyon1, 69622 Villeurbanne cedex, France*
[b] *Laboratoire de Physique et Technologie des plasmas, UMR CNRS 7648, Ecole Polytechnique, 91120 Palaiseau, France*

Available online 26 March 2007

Abstract

Volatile organic compound removal from air requires oxidative processes associating high carbon dioxide selectivity like photocatalysis with fast kinetics like non-thermal plasma. A specially designed coupling reactor has been used to investigate the interaction between photocatalysis and non-thermal plasma. Acetylene has been selected as a model molecule to evaluate oxidation efficiencies. After determining the oxidative efficiency of both techniques used separately, the coupling of plasma with titania photocatalyst has been performed. The influence of UV-irradiation of a photocatalyst placed inside the discharge by external lamps has been investigated. It is reported that photocatalysis leads to a complete mineralization of acetylene, whereas more than 50% of the carbon balance based on CO and CO_2 is missing when plasma alone is performed. The presence of a porous material inside the discharge improves the initial removal rate of acetylene. It tends to favor the formation of adsorbed organic species, indicating that part of plasma reactivity is transferred to the adsorbed phase. Finally, the use of additional external UV-light is reported to improve the formation of carbon dioxide, which means that photocatalysis can be usefully performed in an ionized gas.

Keywords: Dielectric barrier discharge (DBD); Non-thermal plasma; Photocatalysis; Advanced oxidation; VOC

1. Introduction

The removal of volatile organic compounds (VOCs) is one of the main issues of air treatment. Since VOCs are often toxic or irritating, the legislation has become more and more stringent. The first approach consists reducing the emission of VOCs. Nevertheless gaseous wastes cannot be completely avoided. Many organic compounds are strongly odorous or even toxic at concentrations as low as 1 ppmv.

To remove VOCs, various techniques based on adsorption are efficient [1,2], but they consist of pollution transfer from the gaseous phase to a solid surface. Advanced oxidation of VOCs is environmentally safer since VOCs traces are converted to carbon dioxide and water. Catalysis is an efficient mean for organic compound oxidation. Thermally activated catalysts based on noble metal such as Pt and Pd exhibit good perfomances [3–5]. In parallel, photocatalysis has been intensively developed for VOCs elimination during the last 10 years.

Saturated volatile organic compounds advanced oxidation [6–8] as well as unsaturated [9–11] or oxygenated ones [12–14] such as alcohols or ketones, have been intensively studied. Photocatalysis exhibits a high oxidation ability for each type of VOC. Its efficiency has been demonstrated even with a triple carbon–carbon bond, as recently reported by Thevenet et al. [15] for acetylene photocatalytic oxidation.

Dielectric barrier discharge (DBD) has been widely studied first for ozone generation, and nowadays for VOCs oxidation. It is reported as the most hopeful air cleaning technology to remove toxic volatile contaminants in air by Oda et al. [16]. After demonstrating at the end of the 1990s that non-thermal plasma is efficient for organic compounds removal [17,18], the dependance of the VOCs chemical structure on DBD efficiency has been investigated [19]. To improve non-thermal plasma oxidation efficiency, some authors introduced solids into discharges. Porous and high dielectric constant materials were selected. Holzer et al. [20] explored the interaction between plasma and heterogeneous catalysis on Al_2O_3, silica gel and

* Corresponding author. Tel.: +33 4 72 43 62 15; fax: +33 4 72 44 84 38.
E-mail address: chantal.guillard@univ-lyon1.fr (C. Guillard).

0920-5861/$ – see front matter
doi:10.1016/j.cattod.2007.01.057

quartz. Then, Roland et al. [21] widened the scope to $BaTiO_3$, $PbZrO_3$, $PbTiO_3$, and $LaCoO_3$ materials, leading to the conclusion that interaction is mainly governed by the interaction between the plasma phase and the material porosity. Consequently, several packed reactor were developed and studied, screening the variety of VOCs. Benzene [22], toluene, propane [23], and acetaldehyde [24] are the main VOCs investigated. Many studies selected TiO_2 as a very interesting coupling material [22,25–28]. Nevertheless, only very recent studies tried to understand the interaction between plasma and the UV-activated material with a photocatalytic approach [25].

Acetylene has been selected as model pollutant for several reasons. No other study deals with the mineralization of compounds containing triple carbon/carbon bonding. Moreover, acetylene is the simplest alkyne, making reaction intermediates easier to identify and to quantify; carbon balance and reaction pathways get simpler to investigate.

The reasons for coupling plasma photocatalysis are the following: (i) plasma treatment is expected to improve the kinetics of the oxidation reaction, (ii) photocatalysis is expected to improve significantly the carbon dioxide selectivity and the mineralization carbon balance, and (iii) plasma generated UV, due to excited nitrogen relaxation, as well as activated species, are supposed to activate photocatalytic material.

The purpose of this work was to explore and to understand the interaction between non-thermal plasma and titanium dioxide nanoparticles supported on glass fibers. The oxidation capacity for each oxidative technique was separately evaluated. Subsequently, their coupling was explored, with the joint influence of plasma input power and additional external UV-light.

2. Experimental

Coupling of plasma-photocatalysis has been studied in a specially designed Pyrex-glass reactor allowing a plan-to-plan geometry (Fig. 1). The active part of the system consists of rectangular section channel. Two 16 cm^2 copper electrodes are

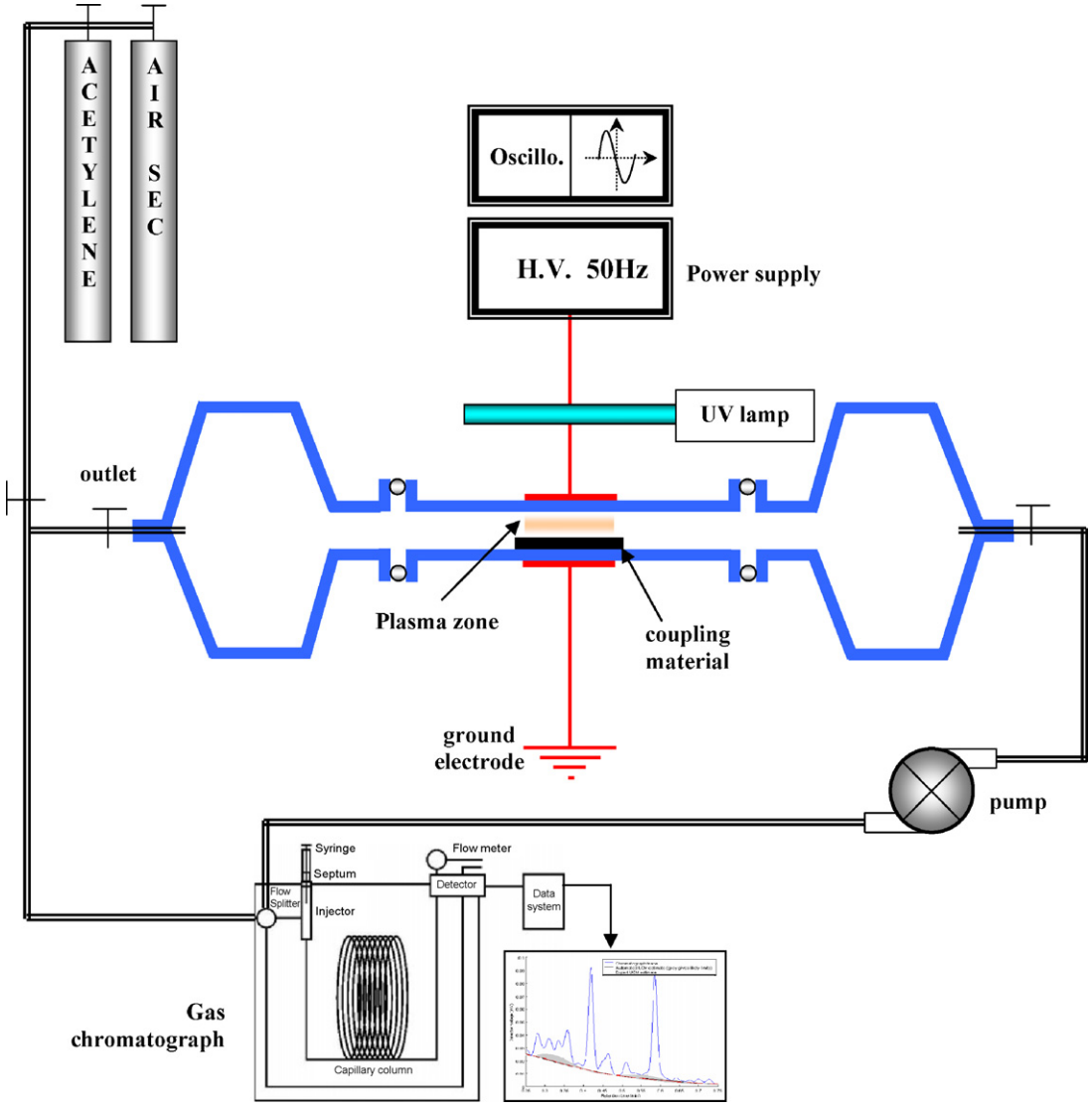

Fig. 1. Scheme of the experimental set up for coupling non-thermal plasma and photocatalysis.

deposited on each side of the largest walls of the channel and connected to a high voltage supply, the volume of the plasma region is 9.6 cm^3, the plasma region length is 2 cm. Glass walls of the channel are both used as dielectric, which drives the discharge to a dielectric barrier discharge mode (DBD). In order to get the discharge, electrodes are submitted to a sinusoidal high voltage ranging from 0 to 25 kV at a 50 Hz frequency. Over the reactor breakdown voltage, (19 kV), energy is transferred to the reactor. The plasma-injected energy is calculated by Lissajou plot method [29,30]. A 2 nF capacitance is place after the dielectric barrier discharge in order to collect charges transferred through the reactor. DBD applied voltage and high capacitance voltage are measured with Lecroy high voltage probes and monitored on Lecroy a Wavesurfer oscilloscope, calculations developed by Manley [29] lead to the precise determination of the input power. The gas gap between the dielectric is 6 mm wide. Dry synthetic air, containing a controlled amount of organic volatile pollutants, can flow through this space. Part of the reactor volume can be filled with two kinds of coated glass fibers. A 16 cm^2 sheet of coated woven glass fibers is deposited on the lower dielectric. The first type of material is only coated with 40 g/m^2 of colloidal silica noted Si40. Its specific area is 28 m^2/g. The second one is coated with 20 g/m^2 of colloidal silica ensuring the fixation of 20 g/m^2 of P25-Degussa titanium dioxide nanoparticles noted Si20Ti20. Its specific area is 20.5 m^2/g. P25-Degussa nanoparticles are 30 nm in diameter, they are made of two titanium dioxide allotropic forms, 80% is anatase, 20% is rutile. During coupling experiments with Si20/Ti20 is the amount of titanium dioxide nanoparticles inside the coupling reactor is 35 mg. The coating process consists in impregnating fibers using industrial size press. Material preparations have been performed by Ahlstrom Research and Services, preparation process is precisely described into Ahlstrom Patent [31]. The photocatalytic material, is cleaned during 30 min under dry synthetic air flow and UV-light before operating. Four external Philips PLL40 UV-lamps are placed around the reactor in order to illuminate Si40 or Si20Ti20 materials, placed in the reactor, from the outer part. Then this set up enables both non-thermal plasma and photocatalytic oxidation of volatile organic compounds.

Experiments have been carried out in a recirculation mode, meaning that the same volume of gas is treated during the whole experiment, the gas goes through the reactor several times. Under those conditions, the evolution of VOC and by-products concentrations can be studied as a function of time and other parameters depending on time like deposited energy. The recirculation flow is 200 mL min^{-1} and is ensured by a pump (Fig. 1). The total volume of the batch reactor is 1.5 L, which leads to a 3 s residence time for a single pass, it means that 7.5 min are needed for a single pass. The analytical system is part of the recirculation system. Gas phase species are monitored with Varian gas phase chromatograph. The system has been especially developed for the experiments. It enables one to perform simultaneously the elution, on a Carbobond column, and the analysis of VOCs as well as those of carbon monoxide and carbon dioxide. Organic species are detected by flame ionization (FID) chromatography, whereas CO and CO_2 are converted into methane over a Ni catalyst in a hydrogen flow, which is analyzed by FID. Acetylene, CO and CO_2 are monitored with a 20 ppm precision. Gases used during the experiments are all provided by Air Liquide. Synthetic air contains less than 0.5 ppm of hydrocarbon and less than 3 ppm of water. Pure acetylene was collected at atmospheric pressure in a cell from a 15 bar tank. After filling the 1.5 L reactor with dry synthetic air at atmospheric pressure, 4.5 mL of pure acetylene are introduced with a gas syringe through a septum inside the coupling reactor, corresponding to a concentration of 3000 ppm of acetylene. U-type helium was used to feed gas-chromatograph column. If coated glass fibers are placed in the reactor, air and acetylene are flowed in the reactor during 1 h to reach adsorption equilibrium. Subsequently, the experiment began.

Four types of experiments have been carried out to understand the interaction between non-thermal plasma and photocatalytic material:

(1) *Photocatalysis*: Si20Ti20 materials are placed inside the reactor and the four UV-lamps are on, no voltage is applied, no discharge is obtained.
(2) *Plasma*: no material is placed in the reactor, and no UV-lamp is on. Dielectric barrier discharge is the only oxidative process performed. The plasma-injected energy has been adjusted to two different input powers (0.22 and 0.32 W) in order to evaluate its influence on acetylene removal.
(3) *Plasma + material*: fiber coated material is placed inside the reactor, no UV-lamp is on. These experiments have been performed with Si40 and Si20Ti20 materials. Two input powers have been studied: 0.22 and 0.32 W.
(4) *Plasma + irradiated material*: these experiments have been performed using Si40 and Si20Ti20 materials. UV-lamps are on in order to evaluate their influence on plasma reactivity: and the possibility of material activation inside the discharge. Two input powers have been studied: 0.22 and 0.32 W.

Adsorbed acids on porous Si40 and Si20Ti20 solids placed inside the discharge during coupling experiments have been analyzed by HPLC. It consists in a Varian ProStar device equipped with Sarasep-Car-H column to perform acids separation. Detection is ensured by UV absorption at 210 nm. First, a 1 h extraction, including a 5 min sonication, is performed on Si40 and Si20Ti20. The extraction solution consists in a pH 2 H_2SO_4 solution corresponding to HPLC device eluent. This procedure was characterized by first extraction coefficients ranging from 92% to 97% for all the acids and supports considered. Gas phase analysis method has been especially developed for gaseous acids. It consists in an acids solubilization into pure water. Bubblers containing pure water are placed on line the reactor after the discharge, they have only been used on line for special analyses experiments, and are removed for usual experiments. Water samples are analyzed by HPLC too.

3. Results

First, results dealing only with acetylene removal are presented and analyzed. Then results concerning carbon monoxide, carbon dioxide and other by-products are reported and discussed.

3.1. Acetylene removal

3.1.1. Coupling 0.22 W non-thermal plasma and photocatalysis, influence of material nature and UV-light

Fig. 2 reports the evolution of acetylene concentration as a function of time corresponding to the four oxidation conditions described above.

The main observation is the slow kinetics of photocatalysis regarding plasma process. Plasmas performed for this part of the experiments are 0.22 W. The initial degradation rate of acetylene is 50 ppm/min with the photocatalytic process, whereas it reaches 190 ppm/min with plasma process. The presence of Si20Ti20 coated glass fibers inside the discharge modifies the initial degradation rate, which is improved of $14 \pm 1\%$ and reaches 215 ppm/min for plasma coupled with Si20Ti20, later called plasma + Si20Ti20. Acetylene degradation rate reaches 250 ppm/min if Si20Ti20 material is irradiated inside the discharge. This process is noticed in the following as plasma + Si20Ti20 + UV. The presence of a solid inside the dielectric barrier discharge modifies the parameters of the discharge. The capacity of the DBD slightly decreases from 4.2 pF for an empty reactor to 4.0 pF when coated glass fiber based photocatalyst is introduced between the electrodes. Then, the 19 kV breakdown voltage is nearly 1 kV lower. Precise study of the influence of such dielectric material placed inside DBD has been intensively studied by Guaitella et al. in 2005 [32]. Consequently, all plasma experiments have been performed at constant input power by adjusting the applied voltage. The increase of initial degradation rate noticed when material is placed in the discharge is not due to an increase of plasma input power but to effective improvement of plasma reactivity. This phenomenon has already been observed and reported by various authors studying the interaction between plasma and catalyst or photocatalyst. Kim et al. [28] suggest that material surface, especially titanium dioxide, can be activated by high-energy particles such as electrons, excited molecules or radicals. Indeed, mean electron energy in similar plasma reactor is 5 eV [33]. Roland et al. [21] suggest that such oxidation improvements are related to the porosity of the structure. Porosity would induce a longer residence time of gas species during diffusion through the solid pore system. They also noticed a significant role of ozone, produced by DBD, interacting with material surface. This hypothesis has to be taken into account with titanium dioxide since a positive effect of ozone on organic compound photocatalytic oxidation is reported [33]. Moreover, as noticed by Kim et al. [28], part of plasma energy is converted into UV-light. Although being small in their intensity, photocatalysis could be performed inside the plasma without classical UV-lamps. In order to determine if plasma UV and excited species activate significantly photocatalytic titanium dioxide particles, experiments have been carried out with the corresponding amount of colloidal silica particles. Results are reported in Fig. 3.

The presence of non-irradiated Si40 or Si20Ti20 materials inside the dielectric barrier discharge induces a similar improvement on the initial degradation rate of acetylene ranging from 12% to 15% in comparison to plasma process alone. This indicates that the nature of the particles deposited on glass fibers does not influence the oxidation efficiency of the system without additional UV-light. The low intensity of UV radiations emitted by plasma species such as metastable nitrogen is not able to activate titanium dioxide particles, even if plasma emission spectrum fits TiO_2 absorption spectrum. Plasma activated species and UV radiations are not able to activate photocatalytic material. Consequently, the improvement observed on acetylene removal is only related to the interaction between plasma and the porous surface independently of the surface chemical nature. This conclusion has been reported with a similar plasma and SiO_2 or TiO_2 device by Chang and Lin [25] about toluene and acetone oxidation. If experiments are carried out with external UV, efficiency remains constant if SiO_2 coated glass fibers are employed. On the contrary, a strong increase is noticed, with additional UV, if titanium dioxide particles are supported on glass fibers. In that case, initial degradation rate is improved by 32%. It represents

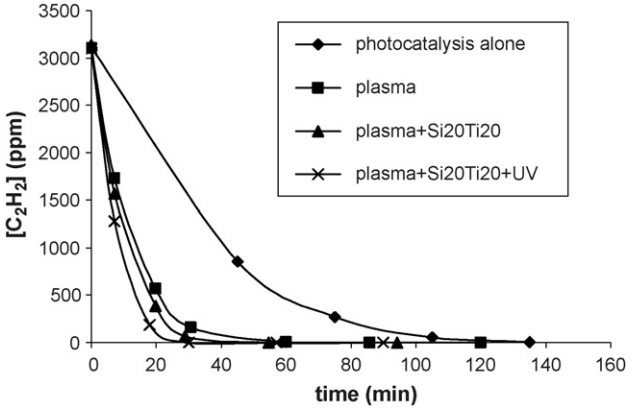

Fig. 2. Evolution of acetylene concentration as a function of time during the four acetylene oxidation processes.

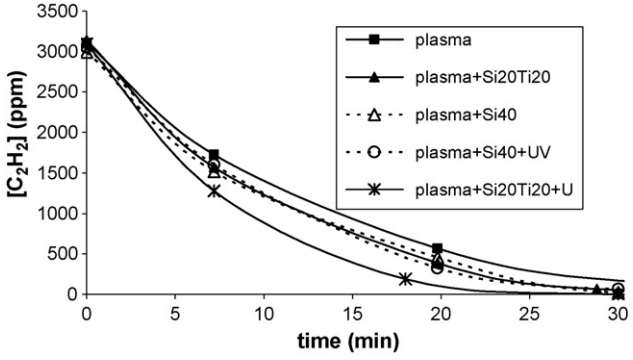

Fig. 3. Evolution of acetylene concentration as a function of time during five different plasma oxidation processes all performed at 0.22 W.

an improvement of 35 ppm of acetylene removed per minute. It means that photocatalysis can be performed into a plasma phase if sufficient UV photons are supplied to the photocatalytic material.

Plasma process induces a much higher initial degradation rate in comparison with photocatalysis. Efficiency can still be improved without any increase of energy consumption when porous material is introduced inside the discharge. The improvement is equivalent with titanium dioxide and silica but the use of additional UV induces a significant photocatalytic effect improving acetylene removal.

3.1.2. Influence of input power

Experiments involving plasma and titanium dioxide have been carried out at two different input powers: 0.22 and 0.32 W. Those experiments aim at evaluating the influence of deposited energy on global acetylene removal efficiency. Results dealing with both energies are reported in Fig. 4a and b.

The increase of 50% of the input power induces a general shift of acetylene degradation curves, for the three plasma conditions, to highest initial degradation rates as reported in Fig. 4a. Acetylene initial degradation rates have been calculated for each oxidation process at both input powers. Values are reported and correlated in Fig. 4b. The comparison between plasma and plasma + Si20Ti20 exhibits and quantifies the improvement relative to the non-irradiated porous surface introduced inside the plasma. The sum of initial degradation rates calculated for photocatalysis and plasma + Si20Ti20 exceeds the value corresponding to plasma + Si20Ti20 + UV showing that no synergy occurs for low energy discharge. At 0.32 W, the interaction between the plasma phase and the porous surface is clearly enforced. The intensity of the interaction phenomenon gets similar to photocatalysis oxidative power. Besides, plasma treatment performed with irradiated Si20Ti20 leads at 0.32 W to a slightly higher initial degradation rate than the cumulative effect of photocatalysis and plasma + Si20Ti20. Nevertheless it can hardly lead to the conclusion of synergism between both techniques since the difference is into the same range than experimental error.

The improvement noticed when TiO_2 is placed inside the discharge, but not irradiated, is only related to the interaction between plasma gas phase and the porous surface. A synergetic effect is observed between non-thermal plasma and photocatalytic oxidation of acetylene performed on irradiated TiO_2. This effect is directly related to plasma-injected energy. In order to perform air cleaning, the removal of the initial pollutant is not the only issue to optimize, attention has to be paid to by-products and final products of the processes.

3.2. By-products and final product formation

As gas phase analysis of acetylene oxidation has been performed by non-thermal plasma and/or photocatalysis carbon monoxide and carbon dioxide are the main detected gaseous by-products. Only traces of carboxylic acid have been detected in the gas phase. On the contrary, various carboxylic acids have been detected in a larger amount, in the adsorbed phase. First, results dealing with organic intermediates are presented. Then results dealing with carbon monoxide and carbon dioxide formation are discussed.

3.2.1. Organic intermediates analysis

Organic intermediates adsorbed on the material placed inside the discharge cannot be easily detected because of the increasing deposited energy in the batch reactor. Nevertheless, those species can give interesting pieces of information on plasma and plasma/material reactivity. Parallel experiments have been carried out under gas flow to favor intermediates formation. In order not to introduce another porous solid inside the discharge, which would have modified its reactivity, adsorbed species have been directly analyzed on coated glass fibers employed for coupling experiments. Analytical procedure is described above in Section 2. Seven different carboxylic acids containing one, two or four carbon in their structures have been identified on each support when plasma is performed (Table 1). This means that the nature of the support does not influence the variety of acids. Moreover, the presence of acids composed by four carbon atoms indicates that plasma reactivity

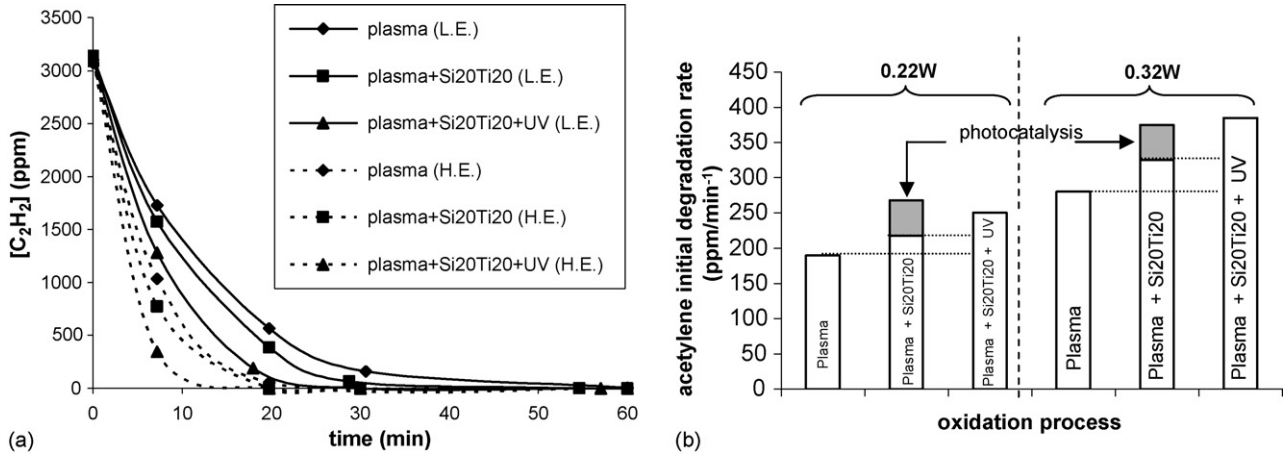

Fig. 4. (a) Evolution of $[C_2H_2]$ as a function of time during three oxidative plasma processes performed at two input powers: 0.22 W (low energy, L.E.) and 0.32 W (high energy, H.E.). (b) Evolution of acetylene initial degradation rate as a function of oxidation process at two different input powers: 0.22 W and 0.32 W.

Table 1
Carboxylic acids detected in the gas phase and the adsorbed phase during acetylene oxidation as a function of the oxidation process

Acids	Photocatalysis	Plasma + Si20Ti20 or plasma + Si20Ti20 + UV	Plasma
Oxalic acid	×	×	
Diglycolic acid		×	
Glycolic acid		×	
Formic acid	×	×	×
Acetic acid	×	×	
Fumaric acid		×	
Butyric acid		×	

can lead to recombination of organic activated species. Photocatalytic process lead to a small amount and a reduced variety of adsorbed acids (Table 1), corresponding to the completion of its carbon balance. Gas phase analysis experiments indicate that traces of formic acid is present in the gas phase (Table 1). Further investigation could lead to a better understanding of plasma/photocatalysis reaction pathways.

3.2.2. Comparison of photocatalytic and plasma processes for CO and CO_2 formation

In Fig. 5, the evolution of CO, CO_2 and C_2H_2 contribution into the carbon balance is reported as a function of time. For the experiment dealing with photocatalysis, carbon monoxide concentration starts to increase until reaching a maximum of 570 ppm, corresponding almost to 10% of the carbon balance, and then decreases slowly. As reported in Fig. 5 and by the authors [15], carbon monoxide is a by-product of acetylene photocatalytic oxidation. One possible way to get CO_2 from acetylene is to consider CO as an intermediate of the degradation pathway. Moreover, since CO_2 initial formation rate is superior to zero, a second way, directly leading from C_2H_2 to CO_2, exists. This way is the main one since, as reported by Thevenet [34], the photocatalytic conversion from CO to CO_2 exhibits very low kinetics. Carbon balance is completed as acetylene is removed since the minimum of carbon dioxide and monoxide cumulative carbon balance curve does not undergo

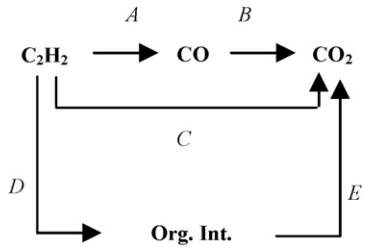

Scheme 1. Kinetics scheme of C_2H_2 oxidation into CO_2 performed by photocatalytic process.

92%. The slight deviation indicates the existence of small amount of intermediates. Some have been identified as carboxylic acids as reported before. This leads us to suggest Scheme 1 in order to describe photocatalytic oxidation of acetylene. Detected organic intermediates are noticed as 'Org. Int.' on the scheme. C is the main kinetics way, on the contrary, A and B, as well as D and E are very minor way in photocatalysis.

The shape of carbon monoxide and carbon dioxide contribution curves into carbon balance is appreciably modified as plasma process is employed (Fig. 6). Plasma oxidation process leads to a sharp maximum relative to carbon monoxide concentration at short reaction time. CO concentration reaches 1120 ppm corresponding to 18% of the carbon balance. Then, CO is rapidly converted into CO_2 once acetylene is completely removed. Carbon dioxide maximum concentration is reduced in comparison to photocatalytic process (Fig. 6). Part of the kinetics scheme proposed by Scheme 1 is still convenient for the reaction. Nevertheless, favored ways are different as plasma is performed. Carbon monoxide is clearly identified as an intermediate between acetylene and carbon dioxide. Even with a slow kinetics, conversion from CO into CO_2 still occurs over 2 h treatment. The fact that CO_2 initial formation rate is superior to zero indicates that even with plasma treatment, a direct way leading from C_2H_2 to CO_2 exists. The presence of traces of gas phase carboxylic acids indicates that those compounds have to be taken into account for a kinetics scheme. Attention has to be paid to the low carbon balance calculated considering carbon dioxide and carbon monoxide. During the

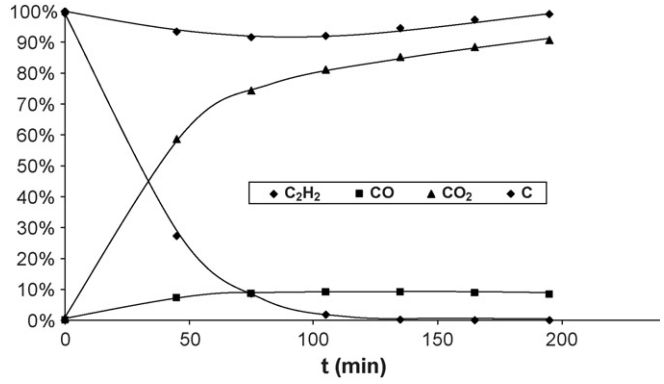

Fig. 5. Evolution of CO, CO_2 and C_2H_2 contribution into carbon balance as a function of time during acetylene photocatalytic oxidation process with Si20Ti20 material.

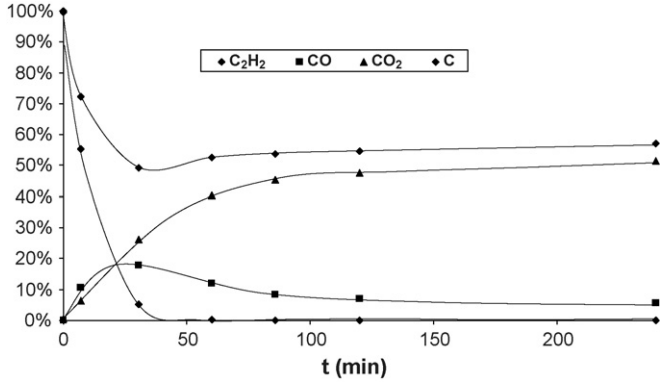

Fig. 6. Evolution of CO, CO_2 and C_2H_2 contribution into carbon balance as a function of time during acetylene oxidation by plasma process (input power: 0.22 W).

first 30 min, carbon balance is tremendously reduced corresponding to the formation of numerous by products. As acetylene is removed it reaches its minimum, 49%. During the following hour of treatment, a 5% improvement is noticed. We suggest that it corresponds to the plasma oxidation of organic by products such as carboxylic acids, which have been identified for those conditions. The equilibrium reached into the batch over 2 h treatment indicates that unidentified carboneous species are produced. First we can suggest that it consists in a polymer deposit, or in a large amount of organic intermediates deposition. But no disactivation of TiO_2 particles is observed when several experiments are carried out. Moreover, if polymerization or a large amount of organic intermediates formation occurred on the material, it would have been further oxidized and removed under plasma oxidative action. But the stationary regime indicates that it is not sensitive to plasma oxidation. Consequently, hypotheses on the formation of deposited carboneous species out of the reactive part of the device can be made. The missing of 45% of the carbon balance would correspond to the formation of at least 4.6 mg of this kind of carboneous compound into our conditions. According to those considerations, Scheme 1 could be modified into Scheme 2 for the plasma process. As plasma oxidation is performed, the main way is A and B. The lack into carbon balance is due to the strong presence of way F. Besides, the direct way C and the successive ways D and E are minor pathways.

3.2.3. *Influence of coupling non-irradiated Si20Ti20 coated fibers with plasma*

If Si20Ti20 material is introduced in the discharge without additional UV, a significant reduction of carbon monoxide formation peak maximum has been noticed (Fig. 7). This phenomenon is not modified if Si20Ti20 coated fibers are UV irradiated (Fig. 8). In presence of Si20Ti20, irradiated or not, CO concentration does not exceed 770 ppm corresponding to 12% of the carbon balance. The maximum is simultaneously reached, at 30 min, into both conditions. Carbon monoxide amount reduction is then only related to the interaction with the porous surface and not with UV induced photocatalytic process. It can be suggested that solid porous surface acts as a meeting point for plasma-activated species. Their residence time is supposed to be increased on the solid surface, consequently, their reactivity would be enhanced. Moreover, from a kinetics point of view, the presence of porous surface could favor way D, which is correlated by the large amount of carboxylic acids observed on material surface, corresponding to 2% of the carbon balance. Consequently, way A would be proportionally reduced, explaining the lowering of CO peak still occurring at same time. As reported in Fig. 7, the presence of non-irradiated TiO_2 coated fibers does not modify the formation of carbon dioxide. The concentration of which get stabilized at the same level than when plasma is performed alone. This indicates that even if way D is favored, plasma oxidation is not able to lead to a significant mineralization of the organic by products. The presence of Si20Ti20 does not significantly modify the carbon balance calculated with carbon monoxide and dioxide. With or without material, the same quantity of missing carbon, is observed. The hypothesis concerning carboneous species deposited out of the active part of the reactor can be made. Consequently, Scheme 2 is still convenient to describe plasma coupled with non-irradiated TiO_2 oxidation process. Nevertheless, the improvement of way D has to be noticed in presence of porous material.

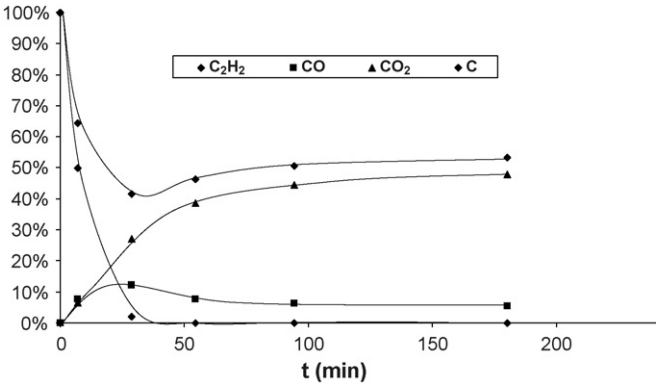

Fig. 7. Evolution of CO, CO_2 and C_2H_2 contribution into carbon balance as a function of time during the oxidation of acetylene by plasma coupled with Si20Ti20 material (input power: 0.22 W).

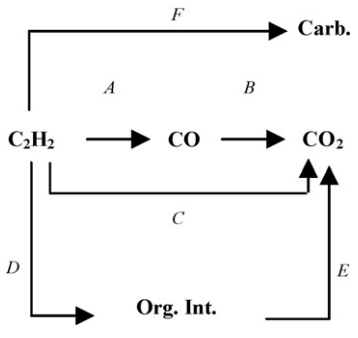

Scheme 2. Kinetics scheme of C_2H_2 oxidation into CO_2 performed by plasma process.

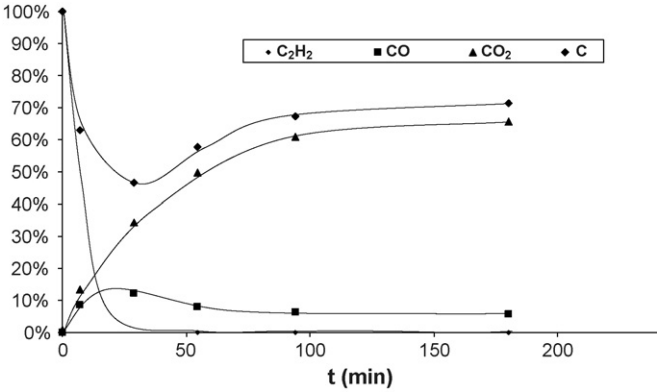

Fig. 8. Evolution of CO, CO_2 and C_2H_2 contribution into carbon balance as a function of time during the oxidation of acetylene by plasma coupled with UV irradiated Si20Ti20 material (input power: 0.22 W).

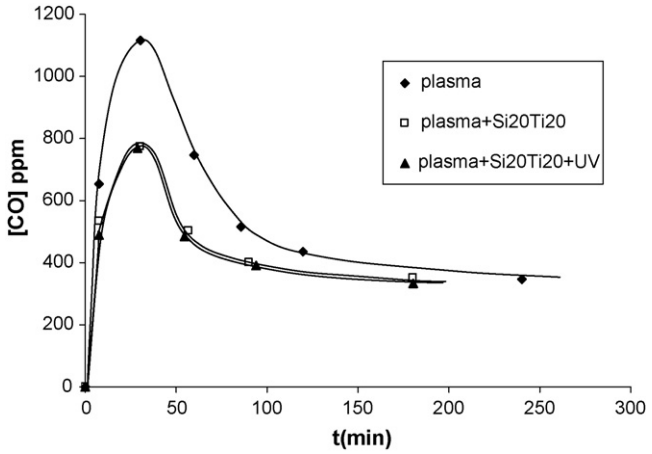

Fig. 9. Carbon monoxide concentration profiles as a function of time during the oxidation of acetylene by (i) plasma, (ii) plasma coupled with Si20Ti20 material, and (iii) plasma coupled with UV irradiated Si20Ti20 material (input power: 0.22 W).

3.2.4. Influence of coupling irradiated Si20Ti20 coated glass fibers with plasma

The influence of external UV on C_2H_2, CO and CO_2 concentration profiles during plasma coupled with Si20Ti20 oxidation process is reported in Fig. 8. Carbon monoxide concentration profile is not modified if UV lamps are added (Fig. 9). Acetylene removal reaction rate is improved by 16% and carbon dioxide formation reaction rate is improved by 90%. This behaviour suggests that UV is able to activate the photocatalytic material placed inside the discharge. Consequently, organic intermediates such as carboxylic acids get oxidized by photocatalytic process leading to the formation of carbon dioxide. Si20Ti20 irradiation favors significantly the kinetics way E, enabling a significant improvement into carbon balance. Nevertheless, more than 25% is missing, hypothesis on carboneous species deposition, organic or not, outside the discharge and the photocatalytic material area, can still be made into these conditions. Consequently, Scheme 2 is still convenient but the kinetics way E is clearly favored as Si20Ti20 material is irradiated.

4. Conclusion

This study improved the understanding of photocatalysis coupled with non-thermal plasma. First, it confirmed that photocatalysis leads to a complete mineralization of acetylene. The main reaction pathway is one step from C_2H_2 to CO_2. On the contrary, non-thermal plasma is not able to mineralize completely acetylene, even if removal characteristic time scales are significantly shorter than in photocatalysis. It is reported that a large part of CO is produced. Moreover, the carbon balance based on CO and CO_2 does not exceed 50%. If porous material is introduced in the discharge, part of the reactivity is transferred into the adsorbed phase, corresponding to the presence of organic intermediates on material surface. Results reported in this article are a first approach, this field appeared to be very interesting from a reaction pathway point of view. Finally, if additional UV are employed, the photocatalytic material is efficiently activated in the plasma phase, a significant activation improvement is noticed for the highest studied plasma input energies. It improves the formation of carbon dioxide, enhancing the carbon balance. Studies at higher input powers have to be carried out since interactions between photocatalytic material and non-thermal plasma seem to be modified as energy range increases.

Acknowledgments

The authors want to thank the French Agency for Environment and Energy Saving (ADEME), CIAT and Ahlstrom Research and Services for their financial and technical support.

References

[1] C. Brasquet, P. Le Cloirec, Carbon 35 (1997) 1307.
[2] M. Popescu, J.P. Joly, J. Carré, C. Danatoiu, Carbon 41 (2003) 739.
[3] N. Cant, W. Hall, J. Catal. 16 (1970) 220.
[4] P. Vernoux, F. Gaillard, L. Bultel, E. Siebert, M. Primet, J. Catal. 208 (2002) 412.
[5] E. Marceau, M. Che, J. Saint-Just, J.-M. Tatibouët, Catal. Today 29 (1996) 415.
[6] D.-S. Mugli, L. Ding, Appl. Catal. B: Environ. 32 (2001) 181.
[7] P. Pichat, J. Disdier, C. Hoang-Van, D. Mas, G. Goutailler, C. Gaysse, Catal. Today 63 (2000) 363.
[8] J.-M. Herrmann, J. Disdier, M.-N. Mozzanega, P. Pichat, J. Catal. 60 (1979) 369.
[9] A. Sirisuk, C.-G. Hill, M.-A. Anderson, Catal. Today 54 (1999) 159.
[10] S. Yamazaki, S. Tanaka, H. Tsukamoto, J. Photochem. Photobiol. A: Chem. 121 (1999) 55.
[11] L. Cao, A. Huang, F.-J. Spiess, S.-L. Suib, J. Catal. 188 (1999) 48.
[12] D.-V. Kovlov, E.-A. Paukshtis, E.-N. Savinov, Appl. Catal. B: Environ. 24 (2000) 7.
[13] J. Arana, J.-M. Dona-Rodriguez, C. Garriga i Cabo, O. Gonzalez-Diaz, J.-A. Herrera-Melian, J. Perez-Pena, Appl. Catal. B: Environ. 53 (2004) 221.
[14] C. Raillard, V. Héquet, P. Le Cloirec, J. Legrand, J. Photochem. Photobiol. A: Chem. 163 (2004) 425.
[15] F. Thevenet, O. Guaïtella, J.-M. Herrmann, A. Rousseau, C. Guillard, Appl. Catal. B: Environ. 61 (2005) 62.
[16] T. Oda, R. Yamashita, I. Haga, T. Takahushi, S. Masuda, J. Electrostat. 57 (2003) 293.
[17] T. Oda, R. Yamashita, T. Takahushi, S. Masuda, IEEE Trans. Ind. Appl. 32 (1996) 118.
[18] T. Oda, IEEE Trans. Ind. Appl. 32 (1996) 227.
[19] S. Futamura, A.-H. Zangh, T. Tamamoto, J. Electrostat. 42 (1997) 51.
[20] F. Holzer, U. Roland, F.-D. Kopinke, Appl. Catal. B: Environ. 38 (2002) 163.
[21] U. Roland, F. Holzer, F.-D. Kopinke, Catal. Today 73 (2002) 315.
[22] H. Kim, A. Ogata, S. Futamura, J. Kor. Phys. Soc. 44 (2004) 1163.
[23] Y.-H. Song, S.-J. Kim, K.-I. Choi, T. Yamamoto, J. Electrostat. 55 (2002) 189.
[24] A. Mizuno, Y. Kisamuki, M. Nogushi, S. Katsura, IEEE Trans. Ind. Appl. 35 (1999) 1284.
[25] C.-L. Chang, T.-S. Lin, Plasma Chem. Plasma Proc. 25 (2005) 227.
[26] S. Futamura, A. Gurusany, J. Electrostat. 63 (2005) 949.
[27] B.-Y. Lee, S.-H. Park, S.-C. Lee, M. Kang, S.-J. Chong, Catal. Today 93 (2004) 769.
[28] H.-H. Kim, Y.-H. Lee, A. Ogata, S. Futamura, Catal. Commun. 4 (2003) 347.

[29] T.C. Manley, in: Proceedings of the 84th General Meeting, New York, 1943.
[30] Z. Falkenstein, J.-J. Coogan, J. Phys. D: Appl. Phys. 30 (1997) 817.
[31] Ahlstrom Patent EP 1069950; AU 735798 US 09/467, 650; JP 2000-542104.
[32] O. Guaitella, F. Thevenet, C. Guillard, A. Rousseau, J. Phys. D: Appl. Phys., submitted for publication.
[33] B.-M. Penetrante, J.-M. Bradley, M.-C. Hsiao, Jpn. J. Appl. Phys. 36 (1997) 5007.
[34] A. Thevenet, Photooxydation catalytique de l'oxyde de carbone en présence d'anatase, Ph.D. Thesis, 1973.